

2A.4 EVALUATION OF CLOUD-RADIATION INTERACTION WITHIN A SINGLE COLUMN MODEL AND REGIONAL CLIMATE MODELING FRAMEWORKS

Suryun Ham, Hoon Park, and Song-You Hong
Department of Atmospheric Science, Global Environmental Laboratory,
Yonsei University, Seoul, Korea

1. INTRODUCTION

It is well known that the cloud-radiation interaction plays a significant role in the forecast skill of the atmospheric models (e.g., Guichard et al. 2002). The vertical distribution of diabatic heating is not only dependent on the latent heating by convective processes but also the radiation process, which is, in turn, affected by clouds. Radiation flux variations determined by cloudiness can lead to a change of temperature profile, which influences the cloud development.

In recent years, cloudiness parameterization related to the cloud-radiation interaction in Global Climate Models (GCMs) has been increasingly developed, ranging from simple diagnostic relations (e.g., Sundqvist 1978; Slingo 1987) to a fully prognostic treatment (e.g., Tiedtke 1993; Tompkins 2002; Larson 2004). If the variance of cloud properties is allowed to vary in a statistical scheme, these schemes can provide a more realistic link between clouds and radiation budget.

The purpose of this study is to understand the importance of the cloud-radiation interaction associated with cloudiness parameterization in a Single Column Model (SCM) and Regional Climate Model (RCM). Sensitivity experiments due to different model physics in each model are designed for a heavy rainfall event.

2. MODEL DESCRIPTION

2.1 Single Column Model

Randall et al. (1996) summarized that when the SCM parameterizations are judged to have performed satisfactorily in tests against observations, they can be transplanted into a three-dimensional atmospheric GCM. As well, they pointed out that it is possible to incorporate an SCM into the framework of a GCM, in which case the SCM parameterizations are available immediately for use in the GCM with little additional work.

The SCM used in this study was developed by Byun and Hong (2006), which is based on a version of NCEP MRF (Kanamitsu et al. 2002). The model

setup and detailed description of the SCM is available in the Byun and Hong. To provide the observational forcing to the SCM, we use the intensive flux array (IFA) data operated in the western equatorial Pacific as part of the Tropical Ocean Global Atmosphere Coupled Ocean-Atmosphere Response Experiment (TOGA COARE), starting from 0000UTC 20 December to 0000 UTC 26 December 1992 (e.g., Ciesielski et al. 2003). This case has been described by Krueger (1997), being the second intercomparison case of Global Energy and Water-cycle Experiment (GEWEX) Cloud System Study (GCSS) working group 4. Several convective episodes occurred during this 6-day period, varying degrees of rainfall intensity. Convection at this time was not well-organized as same as the strong squall line, but the systems had a substantial meso-scale component.

In this study, the SCM is operated in a relaxation mode (Randall and Cripe 1999), where the temperature and moisture profiles are relaxed to the observed profiles using a time constant of 24 hour, as follows McFarquhar et al. (2003). The time integration is performed with 10-min interval, starting from 0000 UTC 20 December. Outputs are taken with 1-hour interval.

2.2 Regional Climate Model

The National Centers for Environmental Prediction (NCEP) Regional Spectral Model (RSM) (Juang et al. 1997) is used in this study. The RSM is a primitive equation model using the sigma-vertical coordinate. The model includes parameterizations of surface, boundary layer (BL), and moist processes that account for the physical exchanges between the land surface, the boundary layer, and the free atmosphere. The simplified Arakawa-Schubert (SAS) scheme (Hong and Pan 1998) is selected to account for the subgrid-scale precipitation processes. The Yonsei University (YSU) Planetary Boundary Layer (PBL) which is a revised non-local vertical diffusion scheme (Hong et al. 2006) and Oregon State University (OSU) Land Surface Model (LSM) scheme (Chen and Dudhia 2001) are used.

RSM domain covers East Asian monsoon region centered over the Korean. The number of grid points in Cartesian coordinates is 109 (west-east) by 86 (north-south). A 50-km resolution is chosen. The RSM vertical resolution employed is 28 layers. The simulation period is summer of 1997 (1 June to 31 August), which includes rainy season over the Korean Peninsula (Fig. 1).

*Corresponding author address: Song-You Hong,
Yonsei University, Department of Atmospheric
Science, Yonsei University, Seoul, 120-749, Korea.
E-mail: shong@yonsei.ac.kr

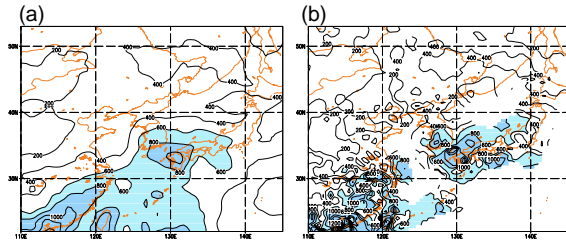


Fig. 1. Monthly mean precipitation (mm/month) averaged for the JJA 1997 obtained from (a) GPCP data and (b) CPC data. Contour intervals are 200 mm, and shaded areas are over 600 mm.

The atmospheric initial and lateral boundary data used in these simulations are NCEP/Department of Energy (DOE) reanalysis II data (Kanamitsu et al. 2002). Model precipitation is compared with the daily Global Precipitation Climatology Project (GPCP) (Huffman et al. 1997) and the Climate Prediction Center (CPC) datasets with a $1^\circ \times 1^\circ$ spatial resolution.

3. EXPERIMENT DESIGN

To evaluate the cloud-radiation interaction, we carried out four experiments in both the SCM and RSM, as seen in Table 1. The CTL experiment is a test with the physics package in section 2. The CPS experiment uses a modified SAS scheme (SAS_qc) in that the conversion profile of clouds to precipitation is modified. The MPS experiment is a test with the WSM3 microphysics scheme for investigating the effect of the microphysics on the cloud-radiation interaction. The RAD experiment is a test of the radiation physics to the cloud-radiation interaction by implementing the WRF radiation schemes, Rapid Radiative Transfer Model (RRTM) long-wave scheme (Mlawer et al. 1997) and Goddard Space Flight Center (GSFC) short-wave scheme (Chou 1992; Chou and Lee 1996), onto the RSM. The effects of partial cloudiness will be examined.

Table 1. Summary of numerical experiments

EXP	Description
CTL	Same physics used in NCEP/DOE reanalysis
CPS	Same as the CTL, except for modified SAS scheme
MPS	Same as the CPS, except for the WSM3 scheme
RAD	Same as the MPS, except for the RRTM and GSFC schemes

4. RESULTS AND DISCUSSION

4.1 Single Column Model

Overall, the temporal evolutions of the surface rainfall show good agreement between all of the experiments and TOGA data, and most of the rainfall is produced due to the convection (Fig. 2). But, all

experiments, underestimate the rainfall amount in general. In addition, the timing of the simulated rainfall is a little late. According to Xu et al. (2003), the timing of the simulated precipitation events for the SCMs agrees with observations much worse than that of the cloud resolving models, because parameterized convection in SCMs is triggered and produces precipitation in a single time step. The quick triggering in the SCMs is related to the large-scale surface fluxes, and the false precipitation events modify the sounding, which impacts the magnitudes of subsequent events.

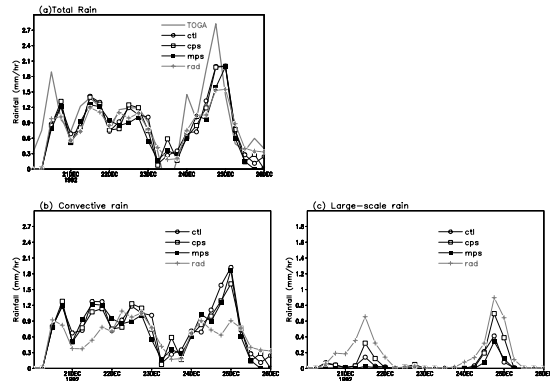


Fig. 2. Time series of the rainfall amount (mm/hour) obtained from TOGA data, CTL, CPS, MPS, and RAD experiments; (a) total rain, (b) convective rain, and (c) precipitation due to the large-scale condensation.

Meanwhile, contributions of each component due to the parameterized convection are different although the total rainfall does not show large differences. In table 2, the CPS experiment is similar to the CTL case in terms of total and convective rainfall amount, whereas the MPS experiment shows the decrease in large-scale rain. Also the RAD experiment shows decrease in convective rain and the increase in large-scale rain.

Table 2. Mean rainfall (mm/day) obtained from each experiment and TOGA data during 0000 UTC 20 to 0000 UTC 26 December 1992, and statistics of the time correlation coefficients (T-Corr).

	Total (mm/day)	Conv.	Larg.	T-Corr
TOGA	23.9			
CTL	20.0	18.9	1.1	0.77
CPS	19.6	17.6	1.9	0.72
MPS	17.9	17.3	0.6	0.68
RAD	19.1	14.9	4.2	0.77

To explain this feature shown in Table 2, we investigate the apparent heat source and moisture sink obtained from the parameterized convection (Fig. 3), as based on the equations of Yannai et al. (1973), for each experiment. Overall, vertical profiles of each experiment show typical convective heating and drying properties. However, their differences are not large, except for the RAD case. The RAD experiment

produces more cooling and moistening in the upper layer, whereas it produces heating and moistening near 800hPa level, compared to the CTL case. Such a gradient between the RAD experiment and the other cases results from difference of the partial cloudiness. The RAD case is calculated by the parameterization of different partial cloudiness from other experiments. As a result, it produces less cloudiness and leads to cooling and moistening in the upper layer. This directly leads to the increase in moisture in the upper troposphere, and the corresponding change in the temperature occurs in the RAD experiment. These changes in convective heating and moisture sink are easily detected in the changes in environmental temperature and moisture fields. On the other hand, it leads to the decrease of temperature near the surface level (Fig. 4).

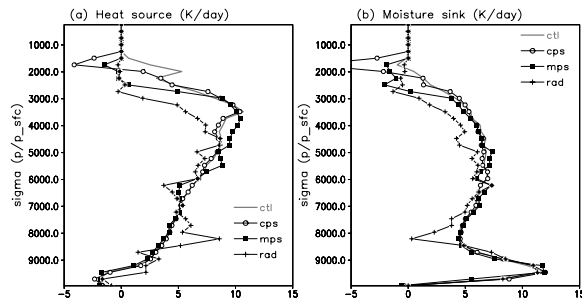


Fig. 3. (a) Apparent heat sources (K/day) and (b) moisture sinks (K/day) obtained from cumulus convections of each experiment. Vertical axis in (a) and (b) denotes the sigma value with surface pressure of 1005hPa. The values are averaged during 6days.

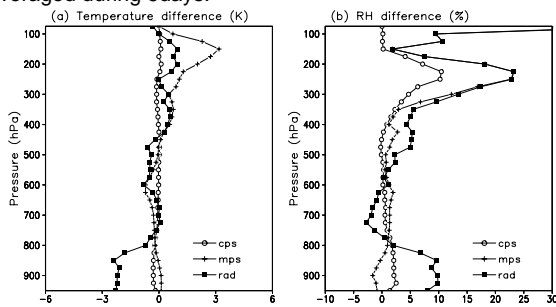


Fig. 4. (a) Temperature (K) and (b) relative humidity (%) differences from the CTL experiment. The values are averaged during 6 days.

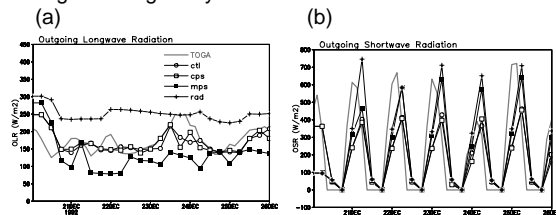


Fig. 5. Temporal variation of the (a) outgoing long-wave flux (Wm^{-2}), and (b) outgoing short-wave radiation flux (Wm^{-2}) at TOA during TOGA COARE period. Gray line indicates the ISCCP C1 flux dataset. Lines with open circle, open square, closed square, and cross symbols are for the CTL, CPS, MPS, and RAD experiments respectively.

Figure 5 shows the time evolution of OLR and

OSR for the TOGA observation and all experiments. Overall, all experiments are underestimated compared to the observation in this period, except for the RAD experiment. But the outgoing radiation fluxes of the RAD experiment are increased, which is due to effects of the less partial cloudiness than other cases in the upper level. Above all, it shows that the outgoing long-wave flux is apparent in the RAD experiment is compared with that from the other cases. It is found that the effect of partial cloudiness and cloud-radiation interaction is important.

4.2 Regional Climate Model

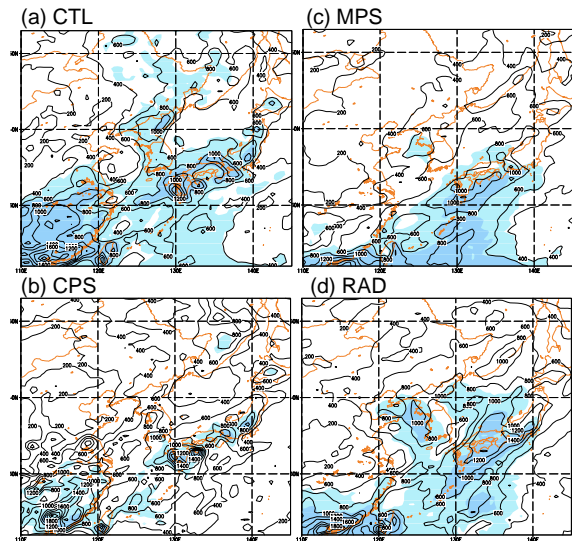


Fig. 6. Monthly mean precipitation (mm/month) averaged for the JJA 1997 obtained from (a) the CTL experiment, (b) the CPS experiment, (c) the MPS experiment, and (d) the RAD experiment. Shaded areas and contoured lines denote the subgrid-scale and total rain, respectively. Shaded areas are over 400mm and intervals are 200mm.

Precipitation is one of the important fields generated during the model simulation. It is also generally held to be the most difficult variable to correctly simulate in a regional model. The simulated monthly rainfall in the 3 months from June to August 1997 is given in Figure 6. Statistics of the simulated precipitation are available in Table 3. Overall, all experiments reproduce the pattern fairly well with comparison to the observation, though the northern precipitation anomalies tend to be larger than that of observation. Results from the CPS experiment are similar to pattern from the CTL case. But total amount of precipitation from the CPS experiment is significantly reduced, in particular, in the portion of the implicit rain. The pattern of precipitation from the MPS case is similar to that of the RAD experiment, whereas the rainfall of the RAD case is increased near the Korean Peninsula when compared with the MPS run. Pattern correlation coefficient of summer mean precipitation anomalies obtained from the MPS

experiment show the highest correlation compared with the other cases. Meanwhile, the RAD run shows that overestimation of the rainfall amount and the lowest pattern correlation coefficient when compared with the other cases.

Table 3. Mean rainfall (mm/hour) obtained from each experiment and GPCP data during JJA 1997, and statistics of the bias (Bias) and pattern correlation coefficients (PC) of simulated precipitation averaged over the whole domain.

	Total (mm/day)	Conv.	Bias	PC
GPCP	4.4			
CTL	4.9	3.7	1.09	0.67
CPS	4.1	2.1	0.91	0.49
MPS	4.6	2.9	1.03	0.79
RAD	4.9	3.2	1.11	0.64

Table 4. Mean flux (Wm^{-2}) averaged over the whole domain for outgoing long-wave radiation flux (OLR), outgoing short-wave radiation flux (OSR), latent heat flux (LH), and sensible heat flux (SH).

	OLR	OSR	LH	SH
RA2	250.8	125.8	80.5	14.8
CTL	270.5	113.9	79.4	17.9
CPS	271.6	115.1	74.7	20.8
MPS	287.3	144.4	72.9	14.5
RAD	214.7	126.0	81.7	32.9

Table 5. Cloud amount averaged over the whole domain for high, middle, low, and total.

	High	Mid	Low	Total
RA2	31.1	22.9	30.3	52.2
CTL	24.2	20.5	18.7	40.6
CPS	24.5	21.1	18.5	42.1
MPS	58.9	32.0	22.5	70.1

Table 4 summarizes the radiation and heat fluxes averaged over the whole domain for the 3 months. Table 5 indicates the cloud amount to high, middle, and low level and total amount. Results of all experiments are represented fairly well when compared with the RA2 datasets. The OLR of all cases except for the RAD experiment is larger than RA2 datasets, whereas that of the RAD run is smaller. The OSR and LH of the RAD case are the most similar to the RA2 datasets, whereas SH is much larger. Fractional amount of clouds affects the short-wave reflection and long-wave emission processes considerably. Difference of the parameterization between the RAD and other runs leads to the changes of these fluxes, whereupon, changing of variable such as temperature is happened.

Figure 7 shows the vertical structures of bias errors of temperature and mixing ratio averaged over the whole domain for 3 months. The result from the

MPS experiment shows that cold bias appears below the 700hPa level, which is due to the increase in cloudiness in the upper troposphere. These biases are more increased in the RAD case. Although temperature of RAD run is smaller than other case, amount of precipitation is increased by keeping up the moistening from the changing in cloudiness.

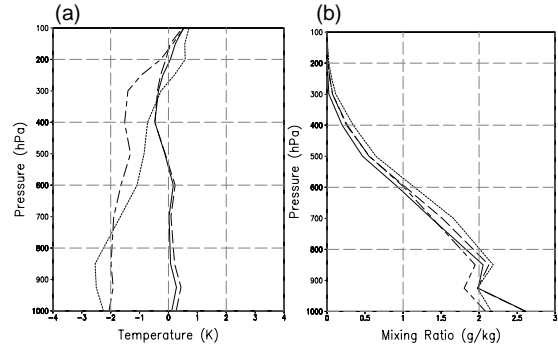


Fig. 7. Bias errors of vertical (a) temperature and (b) Mixing ratio averaged over the model domain for JJA 1997. Solid line for CTL, dashed line for CPS, dotted line for MPS, and dot-dashed line for RAD experiment, respectively.

5. SUMMARY AND CONCLUDING REMARK

This study evaluates the performance of the microphysics and radiation schemes associated with cloud-radiation interaction in both the SCM and RSM. For the evaluation of the partial cloudiness effects, WRF radiation schemes, RRTM long-wave scheme and GSFC short-wave scheme are implemented onto the SCM and RSM.

In the SCM test, the temporal evolutions of the surface rainfall show good agreement between all of the experiments and observation. But all experiments underestimate the rainfall amount in general and the timing of the simulated rainfall is a little late. Meanwhile, the effect of partial cloudiness makes changing of radiation flux such as OLR and OSR. Also, it leads to the diverse vertical distribution of temperature and relative humidity.

In the RCM test, also, all experiments reproduce the pattern fairly well. But the vertical temperature and specific humidity distributions of the MPS and RAD experiments are different from the other cases due to the increase in cloudiness in the upper troposphere. It is found that the effect of partial cloudiness and cloud-radiation interaction on numerical weather prediction is significant.

ACKNOWLEDGEMENTS

This work was funded by the Korea Meteorological Administration Research and Development Program under Grant CATER 2006-2204 and by the Climate Environment System Research Center sponsored by the SRC program of Korea Science and Engineering Foundation.